Solid State Nuclear Magnetic Resonance 141 (2026) 102061

Contents lists available at ScienceDirect

Solid State Nuclear Magnetic Resonance

journal homepage: www.elsevier.com/locate/ssnmr

On the optimal spectral resolution in quadrupole central transition NMR at ultrahigh magnetic fields

Ziyao Peng [a], Xiaolin Wang [b,c], Victor Terskikh [d], Ivan Hung [b], Zhehong Gan [b], Gang Wu [a,*]

[a] Department of Chemistry, Queen's University, 90 Bader Lane, Kingston, Ontario, K7L 3N6, Canada
[b] Center of Interdisciplinary Magnetic Resonance, National High Magnetic Field Laboratory, 1800 East Paul Dirac Drive, Tallahassee, FL, 32310, United States
[c] Department of Chemistry and Biochemistry, California State University East Bay, Hayward, CA, 94542, United States
[d] Metrology, National Research Council Canada, Ottawa, Ontario, K1A 0R6, Canada

ARTICLE INFO

Handling Editor: Prof D Bryce

ABSTRACT

Quadrupole central transition (QCT) NMR has recently been shown to be an effective way of obtaining high spectral resolution for half-integer quadrupolar nuclei in slowly tumbling molecules in liquids. QCT NMR for slowly tumbling molecules shares many common characteristics with conventional CT-based solid-state NMR for half-integer quadrupolar nuclei. As a result, QCT NMR can be considered to be a cousin of solid-state NMR. Experimental QCT NMR data reported so far in the literature strongly indicate that the optimal resolution achievable in QCT NMR increases with the strength of the applied magnetic field (B_0). In this study, we showed that, if the nuclear quadrupole interaction is the predominant relaxation mechanism, the minimal line width (expressed in ppm) obtained in QCT NMR is proportional to B_0^{-3}. In comparison, the corresponding field dependence in CT-based solid-state NMR is only B_0^{-2}. We also demonstrated that the presence of shielding anisotropy (SA) would significantly reduce the B_0^{-3} dependence in QCT NMR. We presented new ^{17}O ($I = 5/2$) QCT NMR results obtained at multiple magnetic fields up to 35.2 T and carefully examined a wide range of previously reported QCT NMR data from the literature for ^{27}Al ($I = 5/2$), ^{39}K ($I = 3/2$), ^{45}Sc ($I = 7/2$), ^{59}Co ($I = 7/2$), ^{71}Ga ($I = 3/2$), and ^{87}Rb ($I = 3/2$) nuclei. Our findings provide a general guideline for future QCT NMR applications especially at ultrahigh magnetic fields.

1. Introduction

In recent years, there have been considerable interests in exploring quadrupole-central-transition (QCT) NMR spectroscopy for half-integer quadrupolar nuclei in slowly tumbling molecules in liquids [1–9]. This is largely because half-integer quadrupolar nuclei are ubiquitous in the Periodic Table but have been hard to study in solution especially for slowly tumbling molecules such as large biological molecules. QCT NMR utilizes the fact that, for half-integer quadrupolar nuclei ($I > 1/2$), only the central transition ($m_I = +1/2 \leftrightarrow -1/2$) displays relatively long transverse quadrupole relaxation times when the molecular tumbling motion is slow (i.e., $\omega_0\tau_c \gg 1$ where ω_0 is the Larmor frequency of the quadrupolar nucleus under study and τ_c is the molecular rotational correlation time) [10–16]. Thus, detection of relatively narrow QCT signals offers an unique opportunity for studying quadrupolar nuclei in slowly tumbling molecules. Since biological macromolecules are naturally slow tumbling in aqueous solution under physiological conditions, QCT NMR can potentially become an effective tool to reveal information unobtainable by conventional spin-1/2 based biomolecular (^{1}H, ^{13}C, ^{15}N, ^{31}P) NMR spectroscopy.

The general spectral features of QCT NMR signals in different motional regimes have been extensively investigated in recent years. In particular, Shen et al. [17] examined how the line width of a QCT NMR signal can be influenced by different relaxation mechanisms including the first- and second-order nuclear quadrupole interactions ($Q^{(1)}$ and $Q^{(2)}$), magnetic shielding anisotropy (SA), and cross-correlation between the SA and second-order quadrupole interactions (SA + $Q^{(2)}$). They showed that the line width generally displays a maximum at $\omega_0\tau_c = 1$ and a minimum in the slow motion regime where $\omega_0\tau_c \gg 1$. For a given system, the minimal line width achievable in QCT NMR depends on the interplay of all abovementioned relaxation mechanisms and the strength of the applied magnetic field. In the literature, all QCT NMR data

This article is part of a special issue entitled: ssNMR above 1 GHz and beyond published in Solid State Nuclear Magnetic Resonance.

* Corresponding author.
E-mail address: wugang@queensu.ca (G. Wu).

https://doi.org/10.1016/j.ssnmr.2025.102061
Received 4 December 2025; Received in revised form 24 December 2025; Accepted 25 December 2025
Available online 26 December 2025

reported so far seem to strongly suggest that the spectral resolution of QCT NMR signals increases with the applied magnetic field. However, a systematic study on this aspect of QCT NMR has not been reported. The objective of the present study is to investigate how the optimal spectral resolution achievable in QCT NMR for half-integer quadrupolar nuclei depends on the strength of the applied magnetic field (B_0). To this end, we collected some new ^{17}O ($I = 5/2$) QCT NMR data at multiple magnetic fields from 11.7 T up to an ultrahigh magnetic field of 35.2 T. In addition, we also carefully examined a wide range of previously reported QCT NMR data from the literature. Examples include ^{27}Al ($I = 5/2$), ^{39}K ($I = 3/2$), ^{45}Sc ($I = 7/2$), ^{59}Co ($I = 7/2$), ^{71}Ga ($I = 3/2$), and ^{87}Rb ($I = 3/2$) QCT NMR data from a variety of chemical and biological systems.

2. Theoretical background

In this section, we will present a brief theoretical background on the optimal spectral resolution achievable in QCT NMR. Our main focus is to examine how the line width of the QCT signal depends on the applied magnetic field, B_0. For a half-integer quadrupolar nucleus with the nuclear spin quantum number of I, the transverse quadrupole relaxation rate due to the first-order quadrupole interaction is known to take the following form [18].

$$R_2^Q = \frac{1}{15}(a\widetilde{\omega}_Q)^2[J(\omega_0) + J(2\beta\omega_0)] \tag{1}$$

where ω_0 is the angular Larmor frequency of the nucleus under observation, and $\widetilde{\omega}_Q$ is known as the reduced angular nuclear quadrupole frequency that is related to the quadrupole parameter (P_Q) in the following fashion:

$$\widetilde{\omega}_Q = \frac{3}{2I(2I-1)}(2\pi P_Q) = \frac{3}{2I(2I-1)}\left(2\pi C_Q\sqrt{1+\eta_Q^2/3}\right) \tag{2}$$

In addition, the two quantities, a and β, are defined as

$$a = \sqrt{I(I+1) - \frac{3}{4}} \tag{3}$$

and

$$\beta = \sqrt{\frac{2}{I(I+1) - \frac{7}{4}}} = \sqrt{\frac{2}{a^2-1}} \tag{4}$$

The spectral density function, $J(\omega)$, in Eq. (1) has the usual definition:

$$J(\omega) = \frac{\tau_c}{1 + (\omega\tau_c)^2} \tag{5}$$

It is important to note the absence of $J(0)$ in Eq. (1) for R_2^Q of QCT as compared to the T_2 relaxation expressions for the satellite transitions and from other nuclear spin interactions.

Previous studies [11,15,19] have shown that, in the slow-motion regime ($\omega_0\tau_c \gg 1$), the second-order quadrupole interaction becomes an important relaxation mechanism and that its contribution to the transverse relaxation (R_2^{Q2}) can be written as:

$$R_2^{Q2} = \frac{149}{63000}\left[\frac{(a\widetilde{\omega}_Q)^2}{\omega_0}\right]^2 J(0) \tag{6}$$

Analog of both the first-order R_2^Q and the second-order R_2^{Q2} contributions can also be found in the two-stage processes of spectral line shape and T_2 relaxation due to molecular dynamics in solids [20,21]. Combining Eqs. (1) and (6), the total line width of the QCT NMR signal (expressed in ppm) is then determined by:

$$\left(\frac{\Delta\nu_{1/2}}{\nu_0}\right)^{QCT} = \left(\frac{R_2^Q}{\pi} + \frac{R_2^{Q2}}{\pi}\right) \Big/ \nu_0 \times 10^6 = \left\{\frac{2}{15}\frac{(a\widetilde{\omega}_Q)^2}{\omega_0}[J(\omega_0) + J(2\beta\omega_0)] + \frac{149}{31500}\left[\frac{(a\widetilde{\omega}_Q)^2}{\omega_0}\right]^2\left(\frac{1}{\omega_0}\right)J(0)\right\} \times 10^6 \tag{7}$$

It can be readily shown that the line width expression given by Eq. (7) reaches a maximum at

$$\tau_c = (\omega_0)^{-1} \tag{8}$$

with

$$\left(\frac{\Delta\nu_{1/2}}{\nu_0}\right)_{max}^{QCT} = \left\{\frac{3a^2+5}{15(a^2+7)}\left(\frac{a\widetilde{\omega}_Q}{\omega_0}\right)^2 + \frac{149}{31500}\left(\frac{a\widetilde{\omega}_Q}{\omega_0}\right)^4\right\} \times 10^6 \tag{9}$$

and a minimum at

$$\tau_c = 5\sqrt{\frac{21}{149}}\,\frac{\sqrt{a^2+7}}{a\widetilde{\omega}_Q} \tag{10}$$

with

$$\left(\frac{\Delta\nu_{1/2}}{\nu_0}\right)_{min}^{QCT} = \frac{1}{150}\sqrt{\frac{149}{21}}\sqrt{a^2+7}\left(\frac{a\widetilde{\omega}_Q}{\omega_0}\right)^3 \times 10^6 \tag{11}$$

It is also important to point out that, when the QCT signal reaches its minimal line width in the slow motion regime $\omega_0\tau_c \gg 1$, the signal position deviates from its true chemical shift position. Under this condition, the signal position (in ppm) is determined by a combination of the isotropic chemical shift (δ_{iso}) and the dynamic frequency shift (δ_d):

$$\delta_{obs}^{QCT} = \delta_{iso} + \delta_d \tag{12}$$

where

$$\delta_d = -\frac{3}{160}\left[\frac{2I+3}{I^2(2I-1)}\right]\left(\frac{P_Q}{\nu_0}\right)^2 \times 10^6 \tag{13}$$

Interestingly, the above expression for δ_d is identical to the isotropic

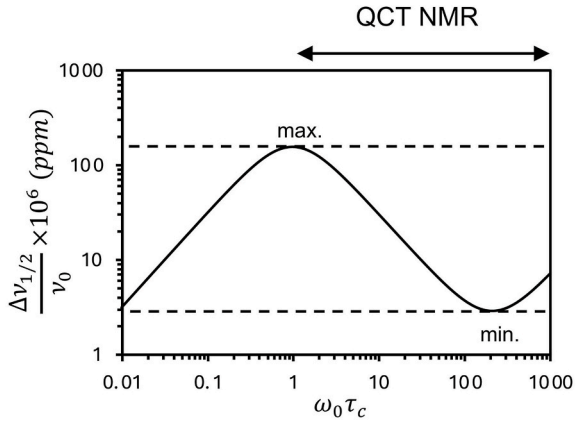

Fig. 1. Theoretical curve displaying the line width (in ppm) of the ^{17}O NMR signal over the entire range of motion. The calculation is based on Eq. (7) and the following NMR parameters are used: $I = 5/2$, $P_Q = 10$ MHz, $\nu_0 = 122$ MHz at $B_0 = 21.1$ T.

value of the second-order quadrupole shift commonly referred to in solid-state NMR [22]. In fact, the origin of the dynamic frequency shift is indeed the isotropic part of the second-order quadrupole interaction. Under the isotropic tumbling condition, the anisotropic part of the second-order quadrupole interaction is averaged to zero.

Fig. 1 displays the general dependence of the QCT line width as a function of $\omega_0\tau_c$. For fast motions where $\omega_0\tau_c \ll 1$, the NMR signal is the sum of all possible single-quantum transitions. This is the region of conventional NMR. In the intermediate ($\omega_0\tau_c \approx 1$) and slow ($\omega_0\tau_c \gg 1$) motions, however, only the QCT NMR signal can be observed in practice. It is interesting to note that, on the basis of Eqs. (9) and (11), the ratio between minimum and maximum line widths is

$$\left(\frac{\Delta\nu_{1/2}}{\nu_0}\right)_{min}^{QCT} \Big/ \left(\frac{\Delta\nu_{1/2}}{\nu_0}\right)_{max}^{QCT} \approx \frac{1}{10}\sqrt{\frac{149}{21}}\,\frac{(a^2+7)^{\frac{3}{2}}}{3a^2+5}\left(\frac{a\widetilde{\omega}_Q}{\omega_0}\right) \tag{14}$$

Using typical values for ^{17}O ($I = 5/2$, $P_Q = 10$ MHz, $\nu_0 = 122$ MHz at $B_0 = 21.1$ T), this ratio is about 0.02. This means that the resolution improvement in QCT NMR in this particular case is approximately 50-fold. This estimate has been confirmed by experimental ^{17}O NMR data of neat glycerol [3]. It is also interesting to note that the ratio given in Eq. (14) displays a weak dependence on the nuclear spin quantum number I in the following fashion:

$$\left(\frac{\Delta\nu_{1/2}}{\nu_0}\right)_{min}^{QCT} \Big/ \left(\frac{\Delta\nu_{1/2}}{\nu_0}\right)_{max}^{QCT} \approx k\left(\frac{P_Q}{\nu_0}\right) \tag{15}$$

where $k = 0.521$, 0.226, 0.152, 0.122, and 0.106 for $I = 3/2$, 5/2, 7/2, 9/2, and 11/2, respectively. Clearly, Eq. (15) also shows an inverse dependence on the applied magnetic field.

Now we turn our attention to the optimal spectral resolution obtainable in QCT NMR. As indicated by Eq. (11), $\left(\frac{\Delta\nu_{1/2}}{\nu_0}\right)_{min}^{QCT}$ displays a B_0^{-3} dependence. This is an extraordinary result and was noted previously [6]. In comparison, the line width (in ppm) of the CT NMR signal obtained with conventional solid-state NMR techniques such as magic angle spinning (MAS) is proportional to B_0^{-2} [22,23]. Thus, QCT NMR should exhibit a higher intrinsic spectral resolution than conventional CT-based solid-state NMR at ultrahigh magnetic fields. This was in fact confirmed by ^{17}O NMR results obtained for the [$^{17}O_4$]oxalate-Al(III)-ovotransferrin complex at 21.1 T [2,24]. However, it is also important to point out the difference between MAS-based NMR for solids and QCT NMR for liquids for quadrupolar nuclei. The residual second-order quadrupole line width in MAS spectra has the B_0^{-2} dependence, but is independent of the SA. The SA is manifested by the presence of spinning sidebands. In QCT NMR, in contrast, the line width is directly influenced by the presence of SA (*vide infra*).

3. Experimental details

All chemicals were purchased from Sigma-Aldrich, unless otherwise stated. Syntheses of [3,5,6-$^{17}O_3$]-D-glucose, [5-^{17}O]-D-glucose, and [^{17}O]nicotinamide were described in previous studies [17,25]. [Rb(*C*222)]Cl was prepared by dissolving RbCl and *C*222 in a 1:1 molar ratio in glycerol. The [^{17}O]nicotinamide sample was prepared by dissolving 74 mg of [^{17}O]nicotinamide in 0.567 g of neat glycerol. The molecular structures of these compounds are shown in the Supporting Information. All NMR data at 11.7, 14.1, and 16.4 T were obtained at Queen's University with standard 5 mm Bruker BBI probes for solution NMR. The general approach to acquire QCT NMR signals is to apply an excitation pulse that is shorter than the conventional 90° pulse by a factor of (I + ½) [6]. Typically, relaxation delays on the order of 10–50 ms were used. NMR data at 21.1 T were collected at the National Research Council Canada (Ottawa) with a Bruker PH BIOPE 5 mm H/X solenoid probe. All NMR data at 28.2 and 35.2 T were acquired on a SCH

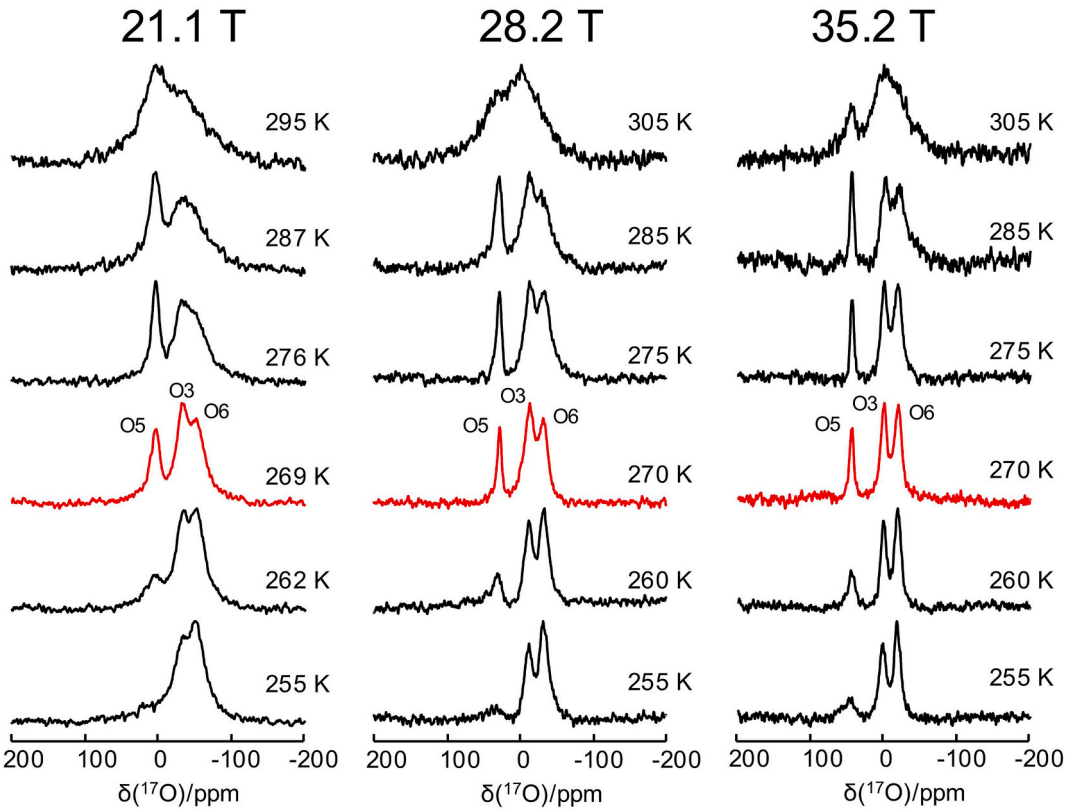

Fig. 2. Variable-temperatures ^{17}O NMR spectra of [3,5,6-$^{17}O_3$]-D-glucose dissolved in glycerol at 21.1, 28.2, and 35.2 T. At each field, the signal with the optimal spectral resolution (i.e., the smallest line width) is highlighted in red. The number of transients collected are 10240 (21.1 T), 8192 (28.2 T) and 2048 (35.2 T). A recycle delay of 10 ms was used in all cases.

magnet with a 3.2 mm HX MAS probe at the National High Magnetic Field Laboratory (Tallahassee, Florida, USA) [26].

4. Results and discussion

Fig. 2 shows the ^{17}O QCT NMR signals from [3,5,6-$^{17}O_3$]-D-glucose dissolved in glycerol obtained at three magnetic fields, 21.1, 28.2, and 35.2 T. At each magnetic field, the spectral resolution of the ^{17}O QCT signals depends critically on sample temperature. While the optimal spectral resolution occurs at the approximately the same temperature (ca. 269–270 K) at the three magnetic fields, a strong field dependence is clearly observed. The drastically improved spectral resolution seen at the ultrahigh magnetic field of 35.2 T is due to a combination of two factors. First, the minimal line width decreases with the applied magnetic field. For example, the smallest line width for the O5 signal is approximately 14 ppm at 21.1 T, which decreases to 8 ppm at 28.2 T and then reduces even further to 5 ppm at 35.2 T (*vide infra*). Second, the chemical shift dispersion increases with the strength of the applied magnetic field. Thus, the resolving power of QCT NMR is significantly enhanced at high magnetic fields.

Fig. 3 shows another example of ^{17}O QCT NMR signals as a function of the applied magnetic field. Here only the ^{17}O QCT NMR signals obtained at the optimal resolution are shown for neat glycerol. Once again, the spectral resolution is drastically improved from 16.4, to 21.1 and to 35.2 T. For example, at 16.4 T, the two ^{17}O QCT NMR signals from the two chemical functional groups of glycerol are severely overlapped, whereas at 35.2 T they are completely resolved. Also as expected, the positions of the ^{17}O QCT signals are shifted towards higher chemical shift values at higher magnetic fields, because of the presence of the so-called dynamic frequency shift. We also observed that, for a given sample, the condition for optimal QCT resolution is less sensitive to sample temperature than the applied magnetic field. Another observation is that the overall sensitivity of the NMR experiment is also drastically enhanced at high magnetic fields. In addition, as seen in Fig. 3, the ^{17}O QCT signals are shifted towards their true isotropic chemical shift positions as the applied magnetic field increases. This is because the dynamic frequency shift is inversely proportional to the square of the applied magnetic field, as predicted by Eq. (13).

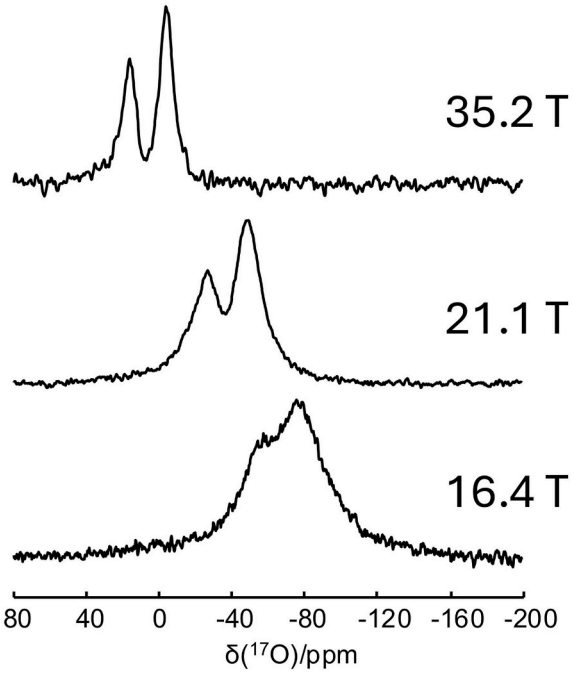

Fig. 3. ^{17}O QCT NMR signals of the optimal resolution for glycerol at 16.4, 21.1, and 35.2 T. All spectra were recorded at 243 K. The number of transients collected is: 1,000,000 (16.4 T), 60,000 (21.1 T), and 20,000 (35.2 T).

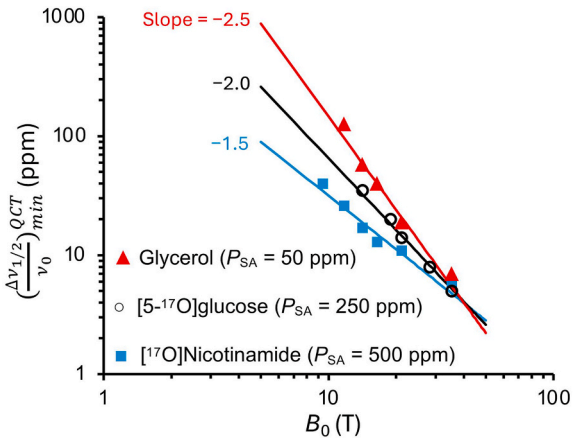

Fig. 4. Experimental ^{17}O QCT NMR data obtained for neat glycerol, [5-^{17}O]-D-glucose dissolved in glycerol, and [^{17}O]nicotinamide dissolved in glycerol showing the minimal line width as a function of the applied magnetic field. The slope of each straight line is given on the plot.

Now we are ready to further quantify the field dependence of the optimal resolution in QCT NMR experiments. Fig. 4 shows extensive ^{17}O QCT data collected for three compounds: neat glycerol, [5-^{17}O]-D-glucose dissolved in glycerol, and [^{17}O]nicotinamide dissolved in glycerol at multiple magnetic fields over a wide range (from 9.4 to 35.2 T). We should point out that ^{17}O QCT data for glycerol at 11.7 and 16.4 T and [^{17}O]nicotinamide at 16.4 T are obtained in the present study whereas all other ^{17}O QCT NMR data shown in Fig. 4 are from the literature [3,17,19]. We observe in Fig. 4 that, for glycerol, the minimal line width data form a good straight line with a slope of −2.5, which is close to the theoretical value of −3 as discussed earlier. For [5-^{17}O]-D-glucose, however, the slope of the straight line is decreased to −2.0, which is further reduced to −1.5 for [^{17}O]nicotinamide. The observed discrepancy among these three compounds can be readily understood on the basis of the ^{17}O SA values in these compounds. Shen et al. [17] showed that the presence of SA would cause additional line broadenings in QCT NMR signals through two relaxation mechanisms: SA itself and SA + $Q^{(2)}$ cross relaxation. As seen in Fig. 4, the reduced field dependence of the optimal resolution in ^{17}O QCT NMR is clearly correlated with the ^{17}O SA values in the three compounds: P_{SA} = 50 ppm in neat glycerol [3], P_{SA} = 200 ppm in [5-^{17}O]-D-glucose [19], and P_{SA} = 500 ppm in [^{17}O]nicotinamide [17]. Here the SA parameter is defined as: $P_{SA} = \left(\sigma_{zz} - \frac{\sigma_{xx}+\sigma_{yy}}{2}\right)\sqrt{1+\eta_{CS}^2/3}$ where σ_{xx}, σ_{yy}, and σ_{zz} are the principal components of the magnetic shielding tensor. However, it is also important to point out that, despite of such a reduced field dependence due to SA, the ^{17}O QCT NMR data shown in Fig. 4 still suggest that a higher magnetic field will result in a better spectral resolution. The extrapolation of the data shown in Fig. 4 indicates that ^{17}O QCT NMR may enter the highly desirable sub-ppm territory at ultrahigh magnetic fields above 70 T. Of course, this kind of ultrahigh magnetic field is not currently available for NMR. However, we should note that, because another parameter that determines the minimal line width of the ^{17}O QCT NMR signal is the value of $P_Q(^{17}O)$, it is still possible to achieve sub-ppm resolution in ^{17}O QCT for oxygen-containing functional groups with relatively small $P_Q(^{17}O)$ values. For example, Eq. (11) predicts that, for $P_Q(^{17}O)$ = 4 MHz such as the PO_4^{3-} group [27], the minimal line width would be only 0.2 ppm at 21.1 T; see Fig. S2 in the Supporting Information. In comparison, the values of $P_Q(^{17}O)$ in neat glycerol, [5-^{17}O]-D-glucose, and [^{17}O]nicotinamide are all greater than 9 MHz.

To further broaden the scope of the present study, we examined all previously reported QCT NMR studies in the literature where multiple magnetic field data are available. In particular, in several pioneering QCT NMR studies, Vogel and co-workers [16,28–32] reported ^{27}Al (I =

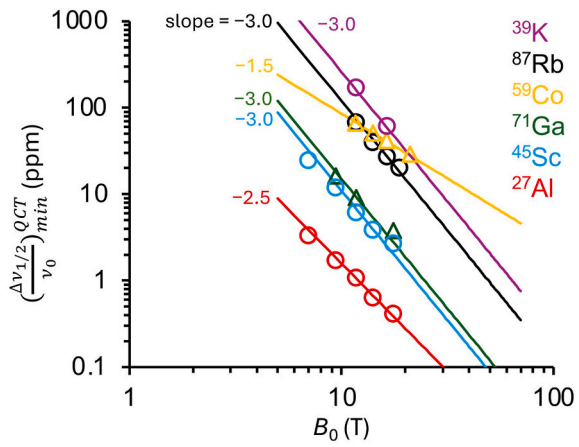

Fig. 5. Experimental line widths of QCT NMR signals as a function of the applied magnetic field. All data were extracted from the literature as quoted in the text. The slope of each straight line is given on the plot.

5/2), ^{71}Ga ($I = 3/2$), ^{45}Sc ($I = 7/2$) QCT NMR data for various transferrin (a 80 kDa protein) samples. More recently, Shen et al. [5] collected ^{59}Co ($I = 7/2$) QCT NMR data for cyanocobalamin (vitamin B_{12}) in glycerol/water mixtures at 11.7, 14.6, 16.4, and 21.1 T. Peng and Wu reported ^{39}K ($I = 3/2$) and ^{87}Rb ($I = 3/2$) QCT NMR results for KCl and Rb[C222]Cl dissolved in glycerol at magnetic fields between 11.7 and 18.8 T [9]. It can be seen from Fig. 5 that most QCT NMR data follow closely the expected B_0^{-3} dependence, except for ^{59}Co. It is well known that SA values are indeed rather small in metal ions such as Al^{3+}, Ga^{3+} and Sc^{3+} and that the metal ion binding to transferrin is tight. In contrast, the ^{59}Co SA value in cyanocobalamin was determined to be very large, P_{SA} = 1250 ppm [5], which is consistent with the value obtained from a single-crystal ^{59}Co NMR study of cyanocobalamin [33]. As a result, the ^{59}Co QCT NMR data for cyanocobalamin shows a much weaker field dependence.

Another factor that can introduce severe line broadenings for QCT NMR signals is chemical exchange. As was shown by a recent ^{23}Na, ^{39}K and ^{87}Rb QCT NMR study [9], when alkali metal ions undergo fast exchange between free and bound states, the averaged QCT NMR signal with the minimal line width is significantly broader than that predicted by Eq. (11). However, despite of this complication due to chemical exchange, the reported QCT data still show better resolution at high magnetic fields.

5. Conclusions

We have conducted a systematic study to examine the optimal spectral resolution achievable in QCT NMR spectroscopy. We found that, in the absence of SA and chemical exchange, the minimal QCT NMR line width (expressed in ppm) displays a remarkable B_0^{-3} field dependence. This suggests that the greatest resolving power of QCT NMR can be realized at ultrahigh magnetic fields. This conclusion is confirmed by experimental QCT NMR data collected for a variety of quadrupolar nuclei having I = 3/2, 5/2, and 7/2 in a wide range of chemical and biological systems. We anticipate that most successful future QCT NMR applications will likely be seen in studies of quadrupolar nuclei that have relatively small SA values and do not undergo fast chemical exchange. It is not difficult to imagine that, in the context of biological systems, best candidates for future QCT NMR studies at ultrahigh magnetic fields may include anions such as Cl^- and cations such as Na^+, K^+, Mg^{2+} and Zn^{2+}. Another advantage of QCT NMR is its simplicity. That is, it does not require any specialized equipment and technique other than a strong magnetic field. Coupled with the sensitivity gain at ultrahigh magnetic fields, it is also possible to develop two-dimensional correlation spectroscopy utilizing QCT NMR signals for slowly tumbling biomolecules.

Declaration of competing interest

The authors declare that they have no known competing financial interests or personal relationships that could have appeared to influence the work reported in this paper.

Acknowledgement

This work was supported by the Natural Sciences and Engineering Research Council (NSERC) of Canada through a discovery grant to GW (RGPIN: 03140-2021). Access to the 21.1 T NMR spectrometer was provided by the Government of Canada Ultrahigh-Field NMR Collaboration Platform, operated by the National Research Council Canada with support from Laboratories Canada, and a consortium of other Canadian Government Departments and Universities. A portion of this work was performed at the National High Magnetic Field Laboratory (NHMFL), which is supported by the National Science Foundation Cooperative Agreement (DMR-2128556, DMR-1644779) and the State of Florida. The NMR user facility at the NHMFL is also supported by NIH RM1GM148766.

Appendix A. Supplementary data

Supplementary data to this article can be found online at https://doi.org/10.1016/j.ssnmr.2025.102061.

Data availability

Data will be made available on request.

References

[1] J. Zhu, I.C.M. Kwan, G. Wu, Quadrupole-Central-Transition ^{17}O NMR Spectroscosy of Protein−Ligand Complexes in Solution, J. Am. Chem. Soc. 131 (40) (2009) 14206–14207, https://doi.org/10.1021/ja906881n.
[2] J. Zhu, G. Wu, Quadrupole central transition ^{17}O NMR Spectroscosy of Biological Macromolecules in Aqueous Soaution, J. Am. Chem. Soc. 133 (4) (2011) 920–932.
[3] J. Zhu, E. Ye, V. Terskikh, G. Wu, Experimental verification of the theory of nuclear Quadrupole relaxati on in liquids over the entire range of molecular tumbling motion, J. Phys. Chem. Lett. 2 (9) (2011) 1020–1023, https://doi.org/10.1021/jz200296g.
[4] R.P. Young, B.G. Caulkins, D. Borchardt, D.N. Bulloch, C.K. Larive, M.F. Dunn, L. J. Mueller, Solution-State ^{17}O Quadrupole Central-Transition NMR Spectroscopy in the Active Site of Tryptophan Synthase, Angew. Chem. Int. Ed. 55 (4) (2016) 1350–1354, https://doi.org/10.1002/anie.201508898.
[5] J. Shen, V. Terskikh, G. Wu, A Quadrupole-Central-Transition ^{59}Co NMR Study of Cobalamins in Solution, ChemPhysChem 20 (2) (2019) 268–275.
[6] G. Wu, ^{17}O NMR studies of organic and biological molecules in aqueous solution and in the solid state, Prog. Nucl. Magn. Reson. Spectrosc. 114–115 (2019) 135–191, https://doi.org/10.1016/j.pnmrs.2019.06.002.
[7] Y. Hinz, J. Beerwerth, R. Böhmer, Anion dynamics and motional decoupling in a glycerol–choline chloride deep eutectic solvent studied by one- and two-dimensional ^{35}Cl NMR, Phys. Chem. Chem. Phys. 25 (41) (2023) 28130–28140, https://doi.org/10.1039/D3CP03668E. DOI.org (Crossref).
[8] Y. Hinz, R. Böhmer, Interplay of ethaline and water dynamics in a hydrated eutectic solvent: Deuteron and oxygen magnetic resonance studies of aqueous ethaline, J. Chem. Phys. 161 (23) (2024) 234504, https://doi.org/10.1063/5.0244255.
[9] Z. Peng, G. Wu, Quadrupole-Central-Transition ^{23}Na, ^{39}K, ^{87}Rb NMR Studies of Alkali Metal Ions under Different Molecular Tumbling Conditions: A Simple Model to Treat Chemical Exchange Involving Qucdrupolar Nuclei, J. Phys. Cqem. A 129 (3) (2025) 803–813, https://doi.org/10.1021/acs.jpca.4c07473.
[10] P.S. Hubbard, Nonexponential Nuclear Magnetic Relaxation by Quadrupole Interactions, J. Chem. Phys. 53 (3) (1970) 985–987, https://doi.org/10.1063/1.1674167. DOI.org (Crossref).
[11] A. Baram, Z. Luz, S. Alexander, Resonance line shapes for semi-integer spins in liquids, J. Chem. Phys. 58 (10) (1973) 4558–4564, https://doi.org/10.1063/1.1679019.
[12] L.G. Werbelow, NMR dynamic frequency-shifts and the quadrupolar interaction, J. Chem. Phys. 70 (12) (1979) 5381–5383.
[13] T.E. Bull, S. Forsen, D.L. Turner, Nuclear magnetic relaxation of spin 5/2 and spin 7/2 nuclei including the effects of chemical exchange, J. Chem. Phys. 70 (6) (1979) 3106–3111..
[14] A. Butler, H. Eckert, Vanadium-51 NMR as a probe of vanadium(V) coorination to human apotransferrin, J. Am. Chem. Soc. 111 (8) (1989) 2802–2809.

[15] L.G. Werbelow, Adiabatic nuclear magnetic resonance linewidth contributions for central transitions of I >1/2 nuclei, J. Chem. Phys. 104 (1996) 3457–3462.
[16] J.M. Aramini, H.J. Vogel, Quadrupolar metal ion NMR studies of metalloproteins, Biochem. Cell. Biol. 76 (2–3) (1998) 210–222.
[17] J. Shen, V. Terskikh, X. Wang, I. Hung, Z. Gan, G. Wu, A Quadrupole-Central-Transition ^{17}O NMR Study of Nicotinamine: Experimentel Evidence of Cross-Relaxation between Second-Order Qudrupole Interaction and Magnetic Shielding Anisotropy, J. Phys. Chem. B 122 (18) (2018) 4813–4820, https://doi.org/10.1021/acs.jpcb.8b02417.
[18] G. Wu, An approximate analytical expression for the nuclear quadrupole transverse relaxation rate of half-integer spins in liquids, J. Magn. Reson. 269 (2016) 176–178.
[19] J. Shen, V. Terskikh, G. Wu, Observation of the second-order quadrupolar interaction as a dominating NMR relaxation mechanism in liquids: the ultraslow regime of motion, J. Phys. Chem. Lett. 7 (17) (2016) 3412–3418.
[20] I. Hung, G. Wu, Z. Gan, Second-order quadrupolar line shapes under molecular dynamics: an additional transition in the extremely fast regime, Solid State Nucl. Magn. Reson. 84 (2017) 14–19.
[21] Y. Dai, I. Hung, Z. Gan, G. Wu, Extending ^{17}O transverse relaxation measurement to satellite transitions as a direct probe of molecular dynamics in solids, Solid State Nucl. Magn. Reson. 137 (2025) 102004, https://doi.org/10.1016/j.ssnmr.2025.102004.
[22] M.H. Cohen, F. Reif, Quadrupole effects in nuclear magnetic resonance studies of solids, Solid State Phys. 5 (1957) 321–438..
[23] A. Samoson, E. Kundla, E. Lippmaa, High resolution MAS-NMR of quadrupolar nuclei in powders, J. Magn. Reson. 49 (2) (1982) 350–357..
[24] J. Zhu, E. Ye, V. Terskikh, G. Wu, Solid-State ^{17}O NMR spectroscopy of large protein-ligand complexes, Angew. Chem., Int. Ed. 49 (45) (2010) 8399–8402, https://doi.org/10.1002/anie.201002041, 10.1002/anie.201002041.
[25] J. Shen, V. Terskikh, J. Struppe, A. Hassan, M. Monette, I. Hung, Z. Gan, A. Brinkmann, G. Wu, Solid-state ^{17}O NMR study of alpha-D-glucose: exploring new frontiers in isotopic labeling, sensitivity enhancement, and NMR crystallography, Chem. Sci. 13 (2022) 2591–2603.
[26] Z. Gan, I. Hung, X. Wang, J. Paulino, G. Wu, I.M. Litvak, P.L. Gor'kov, W.W. Brey, P. Lendi, J.L. Schiano, M.D. Bird, I.R. Dixon, J. Toth, G.S. Boebinger, T.A. Cross, NMR spectroscopy up to 35.2 T using a series-connected hybrid magnet, J. Magn. Reson. 284 (2017) 125–136, https://doi.org/10.1016/j.jmr.2017.08.007.
[27] G. Wu, D. Rovnyak, P.C. Huang, R.G. Griffin, High-Resolution Oxygen-17 NMR spectroscopy of solids by multiple-quantum magic-angle spinning, Chem. Phys. Lett. 277 (1997) 79–83.
[28] J.M. Aramini, M.W. Germann, H.J. Vogel, Field-dependent aluminum-27 NMR studies of the transferrins: an approach for the study of metal ion binding sites in larger proteins, J. Am. Chem. Soc. 115 (21) (1993) 9750–9753.
[29] J.M. Aramini, D.D. McIntyre, H.J. Vogel, Gallium^{3+} binding to ovotransferrin and its Half-Molecules: a multinuclear NMR Study, J. Am. Chem. Soc. 116 (25) (1994) 11506–11511.
[30] J.M. Aramini, H.J. Vogel, A Scandium-45 NMR Study of ovotransferrin and its half-molecules, J. Am. Chem. Soc. 116 (5) (1994) 1988–1993.
[31] M.W. Germann, J.M. Aramini, H.J. Vogel, Quadrupolar metal ion NMR study of ovotransferrin at 17.6 T, J. Am. Chem. Soc. 116 (15) (1994) 6971–6972, https://doi.org/10.1021/ja00094a076. DOI.org (Crossref).
[32] J.M. Aramini, J.A. Saponja, H.J. Vogel, Spectroscopic studies of the interaction of aluminum(III) with transferrins, Coord. Chem. Rev. 149 (1996) 193–229, https://doi.org/10.1016/S0010-8545(96)90026-0.
[33] W.P. Power, C.W. Kirby, N.J. Taylor, A single-crystal Co-59 NMR study of vitamin B-12, J. Am. Chem. Soc. 120 (37) (1998) 9428–9434.